Sketched and truncated polynomial Krylov methods: Evaluation of matrix functions

Davide Palitta¹, Marcel Schweitzer^{2*}, Valeria Simoncini^{1,3}

¹Dipartimento di Matematica, (AM)², Alma Mater Studiorum - Università di Bologna, 40126 Bologna, Italy.

²School of Mathematics and Natural Sciences, Bergische Universität Wuppertal, 42097 Wuppertal, Germany.

³IMATI-CNR, Pavia, Italy.

Contributing authors: davide.palitta@unibo.it; marcel@uni-wuppertal.de; valeria.simoncini@unibo.it;

Abstract

Among randomized numerical linear algebra strategies, so-called sketching procedures are emerging as effective reduction means to accelerate the computation of Krylov subspace methods for, e.g., the solution of linear systems, eigenvalue computations, and the approximation of matrix functions. While there is plenty of experimental evidence showing that sketched Krylov solvers may dramatically improve performance over standard Krylov methods, many features of these schemes are still unexplored. We derive new theoretical results that allow us to significantly improve our understanding of sketched Krylov methods, and to identify, among several possible equivalent formulations, the most suitable sketched approximations according to their numerical stability properties. These results are also employed to analyze the error of sketched Krylov methods in the approximation of the action of matrix functions, significantly contributing to the theory available in the current literature.

Keywords: sketching, randomization, subspace embedding, Krylov subspace method, matrix function, projection method

MSC Classification: 68W20, 65F25, 65F50, 65F60

1 Introduction

The field of numerical linear algebra is currently experiencing a shift of paradigm with the advent of fast and scalable randomized algorithms for many core linear algebra problems, the most prominent one probably being the now widely adopted randomized singular value decomposition [1]. A specific, important tool that has emerged in recent years in the context of randomized numerical linear algebra is the so-called sketch-andsolve paradigm. While initially only used—very successfully—for computations with rather crude accuracy demands, e.g., (low-rank) matrix approximation [2, 3], it was rather recently discovered that—when combined with Krylov subspace methods—it might also be applicable for high accuracy computations as, e.g, the solution of linear systems, eigenvalue computations, and the approximation of matrix functions [4–7]. The main idea in these methods is to use randomized sketching for reducing the cost of orthogonalization by, e.g., combining it with a truncated Gram-Schmidt process. This often allows a huge boost in performance, as orthogonalization is typically the main bottleneck in polynomial Krylov methods when applied to nonsymmetric problems, particularly on modern high-performance architectures, where each inner product introduces a global synchronization point and communication tends to be the dominating factor. For symmetric matrices, computation of an orthogonal Krylov basis is possible by the short recurrence Lanczos method [8], so that the gains one can obtain by reducing the cost of orthogonalization are rather limited. We therefore focus on the nonsymmetric case in the following.

While it was experimentally confirmed that sketched Krylov solvers might dramatically improve performance over standard Krylov methods, many features of these methods are not fully understood yet. In particular, the numerical stability of these methods and how exactly they relate to their non-randomized counterparts needs further analysis. Several recent studies lay a theoretical groundwork with elements of an analysis [5, 6, 9, 10], however, none of these can satisfactorily explain the behavior observed in practice yet, in particular for nonsymmetric problems.

In this work, we derive new theoretical results which help better understand the overall behavior of sketched Krylov methods and identify which of the several possible (mathematically equivalent) formulations of sketched Krylov approximations can be expected to enjoy the most favorable numerical stability properties. We then use these results to analyze the error of sketched Krylov methods for approximating the action of matrix functions, f(A)b, where $A \in \mathbb{R}^{n \times n}$ and $b \in \mathbb{R}^n$, significantly contributing to the currently available theory [5, 6].

One of our main results is a new Arnoldi-type relation for the sketched basis. This is a general result and it can be used to analyze many of the sketching approaches obtained so far, from linear systems to eigenvalue problems. By using this generalization of the Arnoldi relation, the applicability of sketched methods to the solution of matrix Sylvester equations within the Krylov subspace framework can also be explored [11]. The methodology of truncated and sketched Krylov methods has not been used so far in the solution of matrix equations, and our experience is that it requires special care and non-trivial implementations in order to obtain methods which are efficient and at the same time robust and reliable. In the interest of keeping the presentation focused, we postpone the analysis and implementation of Krylov-based matrix

equation solvers to a forthcoming manuscript, which nonetheless fully integrates our general description.

Here is an outline of the paper. In section 2 we recall some background material about the Arnoldi relation (section 2.1) and subspace embeddings (section 2.2) that will serve as a foundation for our analysis. In section 3 we show that a new Arnoldi-like relation, that we name the *sketched Arnoldi relation*, holds also when truncated Krylov subspace methods and sketching techniques are combined. We show the impact of the sketched Arnoldi relation on the construction of a sketched Krylov scheme for matrix function evaluations in section 4. Then, in section 5 we present some general results on functions of certain rank-1 matrix modifications, that will be employed to relate sketched and non-sketched approximations in section 6. The role of eigenvector-related coefficients is further investigated in section 7, leading to the counterintuitive observation that the outlying spurious Ritz values generated by the sketched approach do not contribute to the error vector. In section 8 we discuss some issues related to the stability of the analyzed procedures, while our conclusions are given in section 9.

In the following, the Euclidean norm for vectors and the corresponding induced norm for matrices will be used. The identity matrix will be denoted by I, with dimension clear from the context, while e_j will denote the jth column of the identity matrix. We denote the dth Krylov subspace corresponding to $A \in \mathbb{R}^{n \times n}$ and $b \in \mathbb{R}^n$ by $\mathcal{K}_d(A, b) = \operatorname{span}\{b, Ab, A^2b, \dots, A^{d-1}b\}$. Matlab [12] has been used for all our numerical experiments.

Throughout, exact arithmetic computations will be assumed in our derivations.

2 Background material

In this section we review a few known tools that will be crucial ingredients in our analysis.

2.1 The Arnoldi relation

The backbone of most Krylov subspace methods is the Arnoldi process [13], which, given a matrix $A \in \mathbb{R}^{n \times n}$, a vector $b \in \mathbb{R}^n$, and a target dimension d, computes a nested orthonormal basis $\mathscr{U}_d \in \mathbb{R}^{n \times d}$ of $\mathcal{K}_d(A, b)$ via the modified Gram–Schmidt orthonormalization and gives rise to the Arnoldi relation

$$A\mathcal{U}_d = \mathcal{U}_{d+1}\underline{\mathcal{H}}_d = \mathcal{U}_d\mathcal{H}_d + h_{d+1,d}u_{d+1}e_d^T, \tag{1}$$

where $\underline{\mathscr{H}}_d \in \mathbb{R}^{(d+1)\times d}$, $\underline{\mathscr{H}}_d = [\mathscr{H}_d; h_{d+1,d}e_d^T]$ is an unreduced upper Hessenberg matrix containing the orthogonalization coefficients, and $\mathscr{U}_{d+1} = [\mathscr{U}_d, u_{d+1}]$. The main contributions to the computational cost of performing d steps of the Arnoldi method are d matrix vector products with A at a cost of $\mathcal{O}(d \operatorname{nnz}(A))$ floating point operations (flops), assuming that A is sparse with $\operatorname{nnz}(A)$ nonzeros, and the modified Gram–Schmidt orthogonalization which has a cost of $\mathcal{O}(d^2n)$ flops across all d iterations. Due to its quadratic growth, the cost of orthogonalization quickly dominates the overall cost of the method. In particular, on modern high performance architectures, each inner product introduces a global synchronization point, which leads to a large amount

of communication, unless specific "low-sync" implementations are used, which come with their own challenges regarding numerical stability; see, e.g, the recent survey [14].

2.2 Subspace embeddings

Let \mathcal{V} be a subspace of \mathbb{R}^n . For a given $\varepsilon \in [0,1)$, let $S \in \mathbb{R}^{s \times n}$ be such that for all vectors $v \in \mathcal{V}$,

$$(1 - \varepsilon) \|v\|^2 \le \|Sv\|^2 \le (1 + \varepsilon) \|v\|^2, \tag{2}$$

where $\|\cdot\|$ denotes the Euclidean vector norm. Then S is called an ε -subspace embedding for \mathcal{V} . We can equivalently state the condition (2) in terms of the Euclidean inner product as follows: for all $u, v \in \mathcal{V}$,

$$\langle u, v \rangle - \varepsilon ||u|| \cdot ||v|| \le \langle Su, Sv \rangle \le \langle u, v \rangle + \varepsilon ||u|| \cdot ||v||.$$
 (3)

In practice, one often needs to be able to construct S without any explicit knowledge of the subspace \mathcal{V} (because it is, e.g., a Krylov space that has not been constructed yet). One therefore tries to construct S as a so-called *oblivious* subspace embedding, i.e., one that can be constructed solely knowing the dimension of the subspace \mathcal{V} , but no further information on it [15, Section 8]. Techniques for constructing such oblivious embeddings often use randomization techniques. For instance, it is common to construct S as a randomly subsampled fast Fourier transform (FFT), discrete cosine transform (DCT) or Walsh–Hadamard transform (WHT). To ensure that (2) holds with high probability, the sketching dimension needs to fulfill $s \sim \dim(\mathcal{V})/\varepsilon^2$. Therefore, one typically aims for rather large values of ε in (2), say $\varepsilon = 1/\sqrt{2}$, so that the sketching parameter can be chosen as $s \sim 2 \dim(\mathcal{V})$.

A subspace embedding S induces a semidefinite inner product

$$\langle u, v \rangle_S := \langle Su, Sv \rangle. \tag{4}$$

From the embedding property, it directly follows that when restricted to \mathcal{V} , $\langle \cdot, \cdot \rangle_S$ is an actual inner product; see, e.g., [9, Section 3.1].

In the remainder of the paper, we often simply call S a "sketching matrix", thereby meaning that it is an ε -subspace embedding for a certain Krylov subspace (which will be clear from the context) with a suitable value of ε .

3 The sketched Arnoldi relation

A recently explored avenue for reducing the orthogonalization cost and communication (and possibly storage requirements) in Krylov subspace methods for linear systems is to work with non-orthogonal Krylov bases and impose a "sketched Galerkin condition" with respect to the semidefinite inner product $\langle \cdot, \cdot \rangle_S$ induced by a subspace embedding S to extract approximants from the Krylov space; see, [7] as well as [9] for a discussion of related concepts in model order reduction. Extensions to matrix functions can be found in [5, 6]. To better understand and analyze the behavior of such methods, in the following we derive a sketched analogue of the Arnoldi relation (1).

We consider a truncated Arnoldi procedure, where only the last k vectors are explicitly orthogonalized. We can then use the Arnoldi relation¹

$$AU_d = U_{d+1}\underline{H}_d,\tag{5}$$

with $U_{d+1} = [U_d, u_{d+1}]$, and we recall that \underline{H}_d is banded and that U_d does not need to have all orthonormal columns. In the following we denote $\underline{H}_d = [H_d; h_{d+1,d}e_d^T]$, where only the last component in the last row is nonzero.

Given a sketching matrix S, by means of (5), we can write the sketching SAU_d avoiding its explicit computation. In fact, a more general Arnoldi-type relation for the sketched quantities holds.

Proposition 3.1 Let $SU_{d+1} = Q_{d+1}T_{d+1}$ be a thin QR decomposition with

$$Q_{d+1} = [Q_d, q] \ \ and \ T_{d+1} = \begin{bmatrix} T_d & t \\ 0^T & \tau_{d+1} \end{bmatrix}.$$
 For the sketched method the following Arnoldi-like formula holds:
$$SAU_t = SU_t(H_t + re^T) + \tau_{t+1} \cdot h_{t+1} \cdot re^T$$

$$SAU_d = SU_d(H_d + re_d^T) + \tau_{d+1} h_{d+1,d} q e_d^T, \tag{6}$$

with $r = h_{d+1,d}T_d^{-1}t$ and $q \perp SU_d$.

Proof Le $h^T = h_{d+1,d} e_d^T$. We have

$$SAU_{d} = SU_{d+1}\underline{H}_{d} = Q_{d+1}T_{d+1}\underline{H}Q_{d+1}\begin{bmatrix} T_{d}H_{d} + th^{T} \\ [0^{T}, \tau_{d+1}]\underline{H}_{d} \end{bmatrix}$$

$$= Q_{d}T_{d}(H_{d} + T_{d}^{-1}th^{T}) + \tau_{d+1}qh^{T} = SU_{d}(H_{d} + T_{d}^{-1}th^{T}) + \tau_{d+1}qh^{T}.$$
 (7)
The result follows by inserting the definition of r .

The action of sketching appears only in the vector r and in the scalar τ_{d+1} , while the matrix $H_d + re_d^T$ differs from H_d only in its last column, with a rank-one modification. This will have a quite interesting impact in the following derivations.

To numerically stabilize the sketched procedure, a "basis whitening" process is proposed in [6], which can be seen as a retrospective full orthogonalization of the truncated Krylov basis with respect to the sketched inner product (4). This technique had been used in other earlier sketching-based solvers; see, e.g., [7] and its references. Given a thin QR decomposition $SU_d = Q_d T_d$, in [6] it is proposed to perform the replacements

$$SU_d \leftarrow Q_d$$
, $SAU_d \leftarrow (SAU_d)T_d^{-1}$, $U_d \leftarrow U_dT_d^{-1}$,

where the last replacement is not done explicitly. This procedure was in fact already employed in the derivation of the sketched Arnoldi relation above. The orthogonalization step can be better appreciated by rewriting (7) as

$$SAU_dT_d^{-1} = Q_dT_d(H_d + T_d^{-1}th^T)T_d^{-1} + \tau_{d+1}qh^TT_d^{-1},$$
(8)

¹In the following we use roman font (H_d, U_d) for quantities related to a non-orthogonal Arnoldi relation and calligraphic font $(\mathcal{H}_d, \mathcal{U}_d)$ for quantities related to a fully orthogonal Arnoldi relation.

from which we obtain the whitened-sketched Arnoldi relation (WS-Arnoldi in short)

$$SA(U_d T_d^{-1}) = Q_d(\hat{H}_d + \hat{t}e_d^T) + h_{d+1,d} q e_d^T, \tag{9}$$

where $\hat{H}_d = T_d H_d T_d^{-1}$ and $\hat{t} = (h_{d+1,d}/\tau_d)t$. The transformed basis $U_d T_d^{-1}$ appearing in (9) is orthogonal with respect to the inner product $\langle \cdot, \cdot \rangle_S$ defined in (4) and is known to be extremely well-conditioned also in terms of its condition number. This is stated in the following result, which directly follows from [4, Corollary 2.2]; see also [16, Section 4] for related, earlier results in a probabilistic setting.

Proposition 3.2 If S is an ε -subspace embedding of $\mathcal{K}_d(A,b)$, then the 2-norm condition number of $U_dT_d^{-1}$ is bounded as

$$\kappa_2(U_d T_d^{-1}) \le \sqrt{\frac{1+\varepsilon}{1-\varepsilon}}.$$
(10)

For example, for a practically reasonable embedding quality $\varepsilon = 1/\sqrt{2}$, Proposition 3.2 guarantees that $\kappa_2(U_dT_d^{-1}) \leq 1 + \sqrt{2} \approx 2.4142$.

The inclusion of the orthogonalization coefficients T_d , and thus the use of (9) in place of (6), seems to be very beneficial to the numerical computation. Indeed, computing functions of $H_d + re_d^T$ appears to be quite sensitive to round-off, due to the growing components of r, which lead to poor balancing; see the discussion in Remark 8.2. Note however, that

$$\sqrt{\frac{1-\varepsilon}{1+\varepsilon}}\kappa_2(T_d) \le \kappa_2(U_d) \le \sqrt{\frac{1+\varepsilon}{1-\varepsilon}}\kappa_2(T_d),$$

so that T_d must necessarily be ill-conditioned whenever U_d is ill-conditioned. As U_d results from a truncated orthogonalization process, it will become more and more ill-conditioned as d increases. Despite this fact, inversion of T_d can be expected to not be very problematic in the context of sketched Krylov methods, as we discuss in Remark 8.1.

Remark 3.3 As an alternative to using sketching as means to retrospectively improve the conditioning of a basis that is only locally orthogonal, another recently explored avenue for reducing orthogonalization cost and communication in Krylov methods via sketching is to perform a full Gram-Schmidt orthogonalization, but with respect to the semidefinite inner product $\langle \cdot, \cdot \rangle_S$ defined in (4) instead of the Euclidean inner product; cf., e.g., [4, 5, 10] for use of this technique in the context of solving linear systems by FOM/GMRES or for approximating the action of matrix functions.

4 The impact of the sketched Arnoldi relation

The result of Proposition 3.1 can be used to analyze sketched Krylov methods for the approximation of matrix functions f(A)b. Some first steps regarding the analysis of these methods were done in [6, Section 3.2] and [5, Section 4]. Still, sketched Krylov methods for f(A)b are far from being fully understood from a theoretical perspective. We highlight two particular issues that have not been well explored so far. First, sketching might (and often does) introduce "sketched Ritz values" which lie very far outside the spectral region of A. However, these tend to mostly not negatively influence the performance of the methods. Second, there exist many different formulations for how to compute sketched Krylov approximations, all of them involving computations with potentially very ill-conditioned matrices; cf. also the discussion of the different ways of writing a sketched Arnoldi decomposition presented in section 3. Still, even in the presence of severe ill-conditioning and rank deficiency, sketched Krylov methods often work incredibly well in practice. In this section, we approach both these issues and derive new theoretical results which allow to better capture the properties of these methods and explain the observed behavior.

In our analysis, we compare the full FOM approximation,

$$f_d^{\text{FOM}} = \mathcal{U}_d f(\mathcal{H}_d) e_1 ||b||, \tag{11}$$

based on the Arnoldi decomposition (1), the truncated FOM approximation

$$f_d^{\text{TR}} = U_d f(H_d) e_1 ||b||,$$
 (12)

which is proposed in [5, Algorithm 5] and the "sketched FOM" (sFOM) approximation for f(A)b from [6, Section 2], which is defined as

$$f_d^{SK} = U_d f\left((SU_d)^{\dagger} SAU_d \right) (SU_d)^{\dagger} Sb, \tag{13}$$

where $(SU_d)^{\dagger}$ denotes the Moore-Penrose pseudoinverse of SU_d .

From the sketched Arnoldi relation (6) and the fact that $(SU_d)^{\dagger} = T_d^{-1}Q_d^*$, we directly obtain by straightforward algebraic manipulations that (13) simplifies to

$$f_d^{SK} = U_d f(H_d + r e_d^T) e_1 ||b||, \tag{14}$$

a form much more reminiscent of the standard and truncated FOM approximations (11) and (12). Using the WS-Arnoldi relation (9), we can also write

$$f_d^{SK} = U_d T_d^{-1} f\left(\hat{H}_d + \hat{t}e_d^T\right) e_1 ||Sb||.$$
 (15)

5 Some results on functions of certain rank-one modified matrices

To better understand how the different approximations relate to each other, we begin by stating a quite general result, which provides an explicit relationship between $f(M) \in \mathbb{R}^{d \times d}$ and functions of a rank-one modification of the form $f(M+we_d^T)$. We assume in the following that $M+we_d^T$ is diagonalizable with eigenvalue decomposition

$$M + we_d^T = X\Lambda X^{-1}$$
, where $\Lambda = \operatorname{diag}(\lambda_1, \dots, \lambda_d)$, (16)

and define the corresponding function

$$g_w(t) = \sum_{i=1}^{d} \alpha_i \beta_i f[t, \lambda_i], \tag{17}$$

where

$$f[t,\lambda] = \begin{cases} f'(t), & \text{if } t = \lambda, \\ \frac{f(t) - f(\lambda)}{t - \lambda}, & \text{otherwise,} \end{cases}$$

denotes a divided difference and $\alpha_i = e_d^T X e_i$, $\beta_i = e_i^T X^{-1} e_1$ with X from the eigenvalue decomposition (16). The subscript in g_w is meant to keep track of the rank-one modification used to generate the spectral quantities defining g_w .

Theorem 5.1 Let $M + we_d^T$ have the eigendecomposition (16) and assume that f is defined in a region containing the eigenvalues of M and $M + we_d^T$. Then

$$f(M + we_d^T)e_1 - f(M)e_1 = g_w(M)w,$$

where g_w is defined in (17).

Proof We follow the steps in [17, Theorem 2.1]. We first write

$$(zI - M - we_d^T)^{-1}e_1 - (zI - M)^{-1}e_1$$

$$= (zI - M)^{-1}[(zI - M)(zI - M - we_d^T)^{-1}e_1 - e_1]$$

$$= (zI - M)^{-1}w [e_d^T(zI - M - we_d^T)^{-1}e_1].$$

Using the eigendecomposition of $M + we_d^T$, we have

$$e_d^T (zI - M - we_d^T)^{-1} e_1 = \sum_{i=1}^d \frac{\alpha_i \beta_i}{z - \lambda_i}.$$

Let Γ be a closed curve enclosing the eigenvalues of $M + we_d^T$ and of M. Then

$$f(M + we_d^T)e_1 - f(M)e_1$$

$$= \frac{1}{2\pi i} \int_{\Gamma} f(z) \left((zI - M - we_d^T)^{-1} e_1 - (zI - M)^{-1} e_1 \right) dz$$

$$= \frac{1}{2\pi i} \int_{\Gamma} f(z) (zI - M)^{-1} w (e_d^T (zI - M - we_d^T)^{-1} e_1) dz$$

$$= \frac{1}{2\pi i} \sum_{i=1}^d \alpha_i \beta_i \int_{\Gamma} f(z) \frac{1}{z - \lambda_i} (zI - M)^{-1} dz \ w$$
(18)

$$= \sum_{i=1}^{d} \alpha_i \beta_i f[M, \lambda_i] w$$

$$= g_w(M) w, \tag{19}$$

where we used the contour integral representation of divided differences (see, e.g., [18, Eq. (51)]) in the second to last equality.

Remark 5.2 We note that in [19, Lemma 2.2] a conceptually different representation for rank-one updates of matrix functions was found—also based on the integral representation (18)—but that this representation is less useful for our analysis.

The formula derived in Theorem 5.1 provides insightful information on the role of the (undesired) eigenvalues of the reduced sketched matrix; see section 7. However, as already stated in [17], this expression for the matrix function g_w makes it difficult to analyze and measure the error between the different function evaluations. The following results, based on the same mathematical tools, lead to a more penetrating interpretation, and they may be read off as a different definition of g_w .

Theorem 5.3 Let M be upper Hessenberg and let $\mathbf{m}_d := \prod_{j=1}^{d-1} M_{j+1,j}$. Under the same other hypotheses as in Theorem 5.1, and assuming that all eigenvalues $\{\lambda_1, \ldots, \lambda_d\}$ of $M + we_d^T$ are simple, it holds

$$f(M + we_d^T)e_1 - f(M)e_1 = m_d \sum_{i=1}^d \frac{1}{\omega'(\lambda_i)} f[M, \lambda_i] w,$$
 (20)

from which it also holds

$$f(M + we_d^T)e_1 - f(M)e_1 = \mathbf{m}_d f[M, \lambda_1, \dots, \lambda_d]w, \tag{21}$$

where $f[M, \lambda_1, \dots, \lambda_d]$ is the order-(d+1) divided difference of the function f.

Proof Following the proof of Theorem 5.1, formula (18) dwells with the quantity

$$\mathcal{E} := \int_{\Gamma} f(z)(zI - M)^{-1} w(e_d^T (zI - M - we_d^T)^{-1} e_1) dz.$$

For $M \in \mathbb{R}^{d \times d}$ upper Hessenberg, using the Cayley–Hamilton theorem, we have

$$e_d^T (zI - M - we_d^T)^{-1} e_1 = \prod_{j=1}^{d-1} M_{j+1,j} \prod_{i=1}^d (z - \lambda_i)^{-1},$$

for any $z\in\mathbb{C}$ such that the left-hand side inverse exists. We can thus write the previous integral as

$$\mathcal{E} = \prod_{j=1}^{d-1} M_{j+1,j} \int_{\Gamma} \frac{f(z)}{\omega(z)} (zI - M)^{-1} w dz, \qquad \omega(z) = \prod_{i=1}^{d} (z - \lambda_i).$$

To obtain (20), we write the partial fraction expansion of $1/\omega(z)$, that is

$$\frac{1}{\omega(z)} = \sum_{i=1}^{d} \frac{1}{\omega'(\lambda_i)} \frac{1}{z - \lambda_i},$$

where the prime denotes differentiation of $\omega(z)$ with respect to z, yielding

$$\int_{\Gamma} \frac{f(z)}{\omega(z)} (zI - M)^{-1} w dz = \sum_{i=1}^{d} \frac{1}{\omega'(\lambda_i)} \int_{\Gamma} \frac{f(z)}{z - \lambda_i} (zI - M)^{-1} w dz.$$

Using once again the contour integral representation of divided differences, (see, e.g., [18, Eq. (51)]), and collecting the other terms, the formula (20) is proved.

To obtain (21) we directly use the integral representation in [18, Eq. (51)] in its general form to write

$$\int_{\Gamma} \frac{f(z)}{\omega(z)} (zI - M)^{-1} dz = f[M, \lambda_1, \dots, \lambda_d],$$

or, equivalently, we observe that

$$\frac{1}{2\pi i} \sum_{i=1}^{d} \frac{1}{\omega'(\lambda_i)} f[z, \lambda_i] = f[z, \lambda_1, \dots, \lambda_d],$$

see, e.g., [20, Equation (1.1)].

Remark 5.4 Higher-order divided differences have been used before in matrix function computations, see, e.g., [21, 22], where they are employed for representing the error of the (standard) Arnoldi approximation in the context of restarted methods. As the authors of [21, 22] observe, the numerical computation of higher-order divided differences can quickly become unstable, so that restarted algorithms based on these error representation did not turn out to be universally applicable, in particular not for "hard" problems. Except for [17], where a slightly more stable representation based on first-order divided differences was used, similar to our Theorem 5.1, there has not been too much subsequent work exploring this connection. In [22, Section 4], it is also briefly discussed how to use a divided difference representation in order to estimate the norm of the Arnoldi error when A is (close to) normal.

While it might not be generally useful for numerical computations, in the following we rather use the divided difference representation as a theoretical tool which allows to compare different methods and obtain insight into their qualitative behavior.

A few comments on the previous results are in order. By comparing Theorem 5.1 and (20), it follows that for any $i \in \{1, ..., d\}$ it holds

$$\alpha_i \beta_i = \frac{\prod_{j=1}^{d-1} M_{j+1,j}}{\omega'(\lambda_i)},$$

providing some insight into the magnitude of the product $\alpha_i \beta_i$ for outlying eigenvalues λ_i . In section 7 the role of β_i will be explored in more details.

The results in Theorem 5.3 can be conveniently interpreted by using a matrix analog of the well-known relation between divided differences and differentiation. For an analytic function h defined on the field of values of M, we will also make use of the following bound proved by Crouzeix and Palencia [23],

$$||h(M)||_2 \le (1 + \sqrt{2}) \max_{z \in F(M)} |h(z)|.$$
 (22)

We recall that the field of values of a square matrix $M \in \mathbb{C}^{d \times d}$ is defined as $F(M) = \{z \in \mathbb{C} : z = (x^*Mx)/(x^*x), x \in \mathbb{C}^d\}.$

The following bound can be derived from the *Genocchi–Hermite representation* of divided differences; see, e.g., [18],[24, Appendix B.16],[25, problem (6.1.43)].

Proposition 5.5 Let D be a closed, convex set in the complex plane containing z_1, \ldots, z_{d+1} and let f be analytic on D. Then

$$|f[z_1, \dots, z_{d+1}]| \le \frac{\max_{\zeta \in D} |f^{(d)}(\zeta)|}{d!}.$$

Letting $h = f[\cdot, \lambda_1, \dots, \lambda_d]$, i.e., $h(z) = f[z, \lambda_1, \dots, \lambda_d]$, using (22) and Proposition 5.5, we have the bound

$$||h(M)|| \le (1+\sqrt{2}) \max_{z \in F(M)} |h(z)| \le (1+\sqrt{2}) \frac{\max_{\zeta \in D} |f^{(d)}(\zeta)|}{d!}, \tag{23}$$

where the convex set D now needs to be taken such that it contains both F(M) and the nodes $\lambda_1, \ldots, \lambda_d$ (which are all contained in $F(M + we_d^T)$). We can thus, e.g., take D as the convex hull of $F(M) \cup F(M + we_d^T)$. Then, we can conclude from (21) that

$$||f(M + we_d^T)e_1 - f(M)e_1|| \le m_d(1 + \sqrt{2}) \frac{\max_{\zeta \in D} |f^{(d)}(\zeta)|}{d!} ||w||.$$
 (24)

This type of bound is insightful for functions such as the exponential, for which it is easy to see that the term $m_d/d!$ will eventually go to zero with growing d, while all derivatives $f^{(d)}$ remain bounded. Interestingly, this asymptotic behavior agrees with classical bounds for Krylov subspace approximations for the exponential function [26]. In the next section we will show that the error formulas in Theorem 5.1 and Theorem 5.3 are very general, and can be used to relate the approximation obtained by the fully orthogonal basis with that computed by either the truncated or sketched bases. Hence, the bound in (24), although rather pessimistic in general, ensures that the two quantities $f(M + we_d^T)e_1$ and $f(M)e_1$ will coincide in exact arithmetic, for large enough d.

Example 5.6 We consider the following problem with the Toeplitz matrix M_d , where the subscript stresses the dependence on the dimension d,

```
for d=5:5:30
    M=toeplitz( [-4, 2, zeros(1,d-2)], [-4, 1/2, 1/2, zeros(1,d-3)]);
    rng(21*pi); e1=eye(d,1);
    w=flipud(linspace(1,20,d))'.*randn(d,1);
    Mhat=M+w*[zeros(1,d-1),1];
    y1=expm(M)*e1;
    y1s=expm(Mhat)*e1;
end
```

Figure 1 shows the error norm $\|\exp(M_d + w_d e_d^T)e_1 - \exp(M_d)e_1\|$ and the bound $(1 + \sqrt{2})\|w\|m_d/d!$. Since m_d is moderate, the convergence slope of the asymptotic curve nicely follows that of the true error.

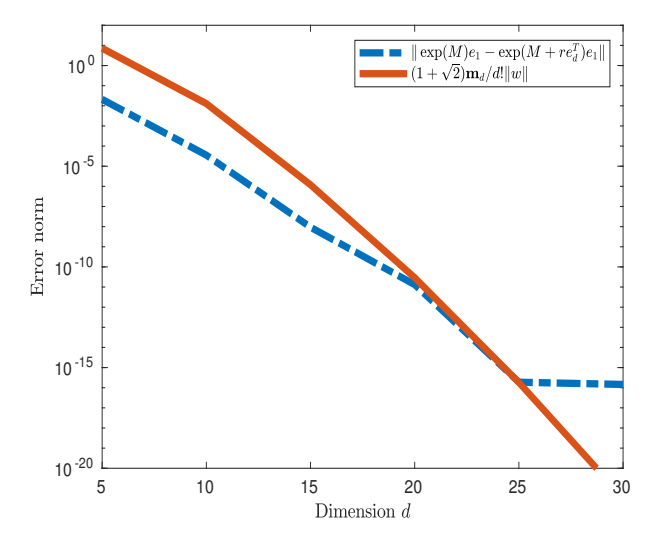


Fig. 1 Example 5.6. True error $\|\exp(M_d + we_d^T)e_1 - \exp(M_d)e_1\|$ (dashed line) as the dimension d grows, and bound $(1 + \sqrt{2})\|w\|m_d/d!$ (solid line).

For functions other than the exponential the bound in (24) may not be significant. As an example, for $z^{-1/2}$ the formula for the derivative contains a factor that essentially grows as the factorial. To provide further insight, we resort to representations involving more general tools that take into account the properties of divided differences in complex domains. More precisely, we can use a result proved by Curtiss in 1962. We first recall that for a bounded region D of the complex plane whose boundary is an admissible Jordan curve, it is possible to define a function $z = \chi(\omega) = \mu\omega + \mu_0 + \frac{\mu_1}{\omega} + \frac{\mu_2}{\omega^2} + \cdots$, where $\mu > 0$ is called the capacity of the Jordan curve, and ω is defined outside the unit circle. The function χ maps conformally the region outside the unit circle into the exterior of \bar{D} . Setting $\omega = r \exp(i\theta)$, there exists a maximum value of r, that is $\rho > 1$, such that f is analytic on the region between the exterior of D and the curve $C_r = \{z = \chi(r \exp(i\theta))\}$, with $\theta \in [0, 2\pi]$. We refer to [20] for a more comprehensive description of the notation.

Theorem 5.7 [20, Theorem 4.1] With the above notation, let D be a bounded region of the complex plane whose boundary is an admissible Jordan curve, and let μ be the capacity of ∂D . Let f be analytic on $C = \bar{D}$ and let the sequence of $\{\lambda_1, \ldots, \lambda_d\}$ be equidistributed on ∂D . Let $\rho > 1$ be the largest value such that f is analytic in the extended curve C_{ρ} containing C. Then for any r, $1 < r < \rho$,

$$|f[\lambda_1,\ldots,\lambda_d]| \le \frac{\ell_{C_r}}{2\pi(\mu r)^d} \max_{z \in C_r} |f(z)|,$$

where ℓ_{C_r} is the length of the curve C_r .

Combining the relations above and using (21), we obtain the following bound, where D can be taken as the convex set above,

$$||f(M + we_d^T)e_1 - f(M)e_1|| \leq m_d(1 + \sqrt{2}) \max_{z \in F(M)} |[z_1, \dots, z_d]f(z)| ||w||$$
$$\sim \ell_{C_r} \frac{m_d}{(\mu r)^d} \max_{z \in C_r} |f(z)| ||w||.$$

Clearly, the above analysis assumes an idealized setting (e.g., in reality, the λ_i will not be equidistributed on ∂D) and additionally, the obtained bound cannot be expected to be sharp and descriptive of the actual difference of the two approximations. It should merely be seen as a first hint at what kind of results might be possible to obtain for general f. However, such more refined results will require advanced tools from complex analysis which are well beyond the scope of the current work.

The analysis above focuses on the role of the considered function, acting on specific spectral domains. The role of w will be discussed in the next section.

6 Error analysis with respect to the FOM approximation

We can now use Theorem 5.1 to relate the different possible sketched and truncated Krylov approximations to each other, as they all result from rank-one modifications of one another. Note that for the sketched Krylov approximation, we will use the representation (14) for analysis purposes (as it directly uses the matrix H_d), although the representation (15) is better suited for actual computations, as we will illustrate in Example 8.3 below. Before stating our results, let us introduce yet another way of writing the sketched or truncated Krylov approximations: As both U_d and \mathcal{U}_d contain nested bases of $\mathcal{K}_d(A,b)$, there exists a nonsingular upper triangular matrix \mathcal{T}_d such that $U_d = \mathcal{U}_d \mathcal{T}_d$; the matrix \mathcal{T}_d can, e.g., be obtained via a Gram-Schmidt based QR decomposition. We write

$$\mathscr{T}_{d+1} = \begin{bmatrix} \mathscr{T}_d & t \\ 0^T & \widehat{\tau}_{d+1} \end{bmatrix}. \tag{25}$$

Using this, we can write the sketched FOM approximation in terms of the orthogonal Krylov basis \mathcal{U}_d as

$$f_d^{\text{SK}} = \mathcal{U}_d f(\mathcal{J}_d H_d \mathcal{J}_d^{-1} + \mathcal{J}_d r e_d^T \mathcal{J}_d^{-1}) \mathcal{J}_d e_1 \|b\|.$$
 (26)

Now, from (5) and the fact that the columns of \mathcal{U}_d are orthonormal it follows by straightforward algebraic manipulations that

$$\mathcal{I}_d H_d \mathcal{I}_d^{-1} = \mathcal{H}_d - h_{d+1,d} \mathcal{U}_d^T u_{d+1} e_d^T \mathcal{I}_d^{-1}.$$

$$(27)$$

Thus, the matrix at which f is evaluated in (26) is a rank-one modification of \mathcal{H}_d . Further simplification is possible by noting that the first columns of U_d and \mathcal{U}_d are

identical, so the top-left entry of \mathscr{T}_d can be chosen to be 1 and furthermore, $e_d^T \mathscr{T}_d^{-1} = e_d^T/\widehat{\tau}_d$. Using these observations together with (27) allows to rewrite (26) as

$$f_d^{\text{SK}} = \mathcal{U}_d f(\mathcal{H}_d + \hat{r}e_d^T) e_1 ||b||, \tag{28}$$

where we introduced the shorthand notation

$$\widehat{r} = (\mathcal{T}_d r - h_{d+1,d} \mathcal{U}_d^T u_{d+1}) / \widehat{\tau}_d$$

$$= (\mathcal{T}_d T_d^{-1} t - \mathcal{U}_d^T u_{d+1}) (h_{d+1,d} / \widehat{\tau}_d)$$

$$= (\mathcal{T}_d T_d^{-1} t - t) (h_{d+1,d} / \widehat{\tau}_d),$$
(29)

with t coming from (25).

By following the same steps for the truncated FOM approximation, we find the representation

$$f_d^{\text{TR}} = \mathcal{U}_d f(\mathcal{H}_d - h_{d+1,d} t e_d^T) e_1 ||b||. \tag{31}$$

Corollary 6.1 The sketched and full Arnoldi approximations f_d^{SK} and f_d^{FOM} from (14) and (11) fulfill

$$f_d^{\text{SK}} - f_d^{\text{FOM}} = \mathcal{U}_d g_{\widehat{r}}(\mathcal{H}_d) \widehat{r} \|b\|, \tag{32}$$

where \hat{r} is defined in (30) and $g_{\hat{r}}$ is defined in (17), with respect to the eigendecomposition of $\mathcal{H}_d + \hat{r} e_d^T$.

Proof The result follows by applying Theorem 5.1 with $M = \mathcal{H}_d$ and $w = \hat{r}$.

Corollary 6.2 The truncated and full Arnoldi approximations f_d^{TR} and f_d^{FOM} from (12) and (11) fulfill

$$f_d^{\text{TR}} - f_d^{\text{FOM}} = \mathscr{U}_d g_v(\mathscr{H}_d) v \|b\|,$$

where $v = -h_{d+1,d}t$ and g_v is defined in (17), with respect to the eigendecomposition of $\mathcal{H}_d + ve_d^T$.

Proof The result follows by applying Theorem 5.1 with $M = \mathcal{H}_d$ and w = v.

There are several possibilities for comparing the sketched and truncated Arnoldi approximations to each other. We present only the one based on the banded Hessenberg matrix H_d and the non-orthogonal basis U_d in the following. It would also be possible, using (28) and (31), to state a result in terms of the matrices \mathcal{U}_d and \mathcal{H}_d from the full Arnoldi process, but this is less appropriate here as neither of the two methods uses these matrices.

Corollary 6.3 The truncated and sketched Arnoldi approximations f_d^{TR} and f_d^{SK} from (12) and (14) fulfill

$$f_d^{\text{TR}} - f_d^{\text{SK}} = U_d g_r(H_d) r ||b||,$$

where g_r is defined in (17), with respect to the eigendecomposition of $H_d + re_d^T$.

Proof The result follows from Theorem 5.1 applied with $M=H_d$ and w=r.

When bounding the distance between the different approximations, the results of Theorem 5.7 and Proposition 5.5 can be used to handle the matrix functions occurring on the right-hand sides of the preceding corollaries by bounding $||g_w(\mathcal{H}_d)||$. Such bounds on the norm of the matrix function are only useful if we also have appropriate bounds available for the vectors w. In the following, we particularly discuss the vector $w = \hat{r}$ from Corollary 6.1 which relates the sketched to the full Arnoldi approximation.

Consider the equation (29). Using the fact that $t = Q_{d+1}^* S u_{d+1}$ together with $T_d^{-1} Q_d^* = (S U_d)^{\dagger}$, we find the representation

$$\widehat{r} = (\mathscr{T}_d(SU_d)^{\dagger} S u_{d+1} - \mathscr{U}_d^T u_{d+1}) (h_{d+1,d}/\widehat{\tau}_d) = \mathscr{U}_d^T (U_d(SU_d)^{\dagger} S u_{d+1} - u_{d+1}) (h_{d+1,d}/\widehat{\tau}_d),$$

where we have used $\mathscr{T}_d = \mathscr{U}_d^T U_d$ for the second equality. The vector $(SU_d)^{\dagger} Su_{d+1}$ appearing above is the solution vector x_S of the sketched least squares problem

$$x_S = \arg\min_{x \in \mathbb{R}^d} ||S(U_d x - u_{d+1})||.$$

From established theory covering sketching methods for least squares problems[2], it is known that the solution x_S of the sketched problem cannot have a significantly higher residual than the solution of the original problem if the embedding quality is high enough. Precisely, denoting by $x_{\star} = U_d^{\dagger} u_{d+1}$ the solution of the non-sketched least squares problem, we have the following inequality relating the residuals of x_S and x_{\star} ,

$$||U_d x_S - u_{d+1}|| \le \sqrt{\frac{1+\varepsilon}{1-\varepsilon}} ||U_d x_{\star} - u_{d+1}||.$$

Further, due to the fact that $U_d = \mathcal{U}_d \mathcal{T}_d$ is a QR decomposition, we have that $\|U_d x_\star - u_{d+1}\| = |\widehat{\tau}_{d+1}|$. Since $\|U_d x_\star - u_{d+1}\| = \|(I - \mathcal{U}_d \mathcal{W}_d^T) u_{d+1}\|$, the quantity $|\widehat{\tau}_{d+1}|$ measures the contribution of the new vector u_{d+1} to the expansion of the Krylov subspace.

Putting all this together and using the fact that \mathscr{U}_d has orthonormal columns, we find

$$\|\widehat{r}\| \le h_{d+1,d} \left| \frac{\widehat{\tau}_{d+1}}{\widehat{\tau}_d} \right| \sqrt{\frac{1+\varepsilon}{1-\varepsilon}}$$
(33)

As long as the space keeps growing, we expect that $\left|\frac{\widehat{\tau}_{d+1}}{\widehat{\tau}_d}\right| \approx 1$, so that an overall result of the following form can be obtained from Proposition 5.5

$$||f_d^{\text{SK}} - f_d^{\text{FOM}}|| \lesssim (1 + \sqrt{2}) \sqrt{\frac{1+\varepsilon}{1-\varepsilon}} ||b|| \frac{\prod_{j=1}^{d-1} \mathscr{H}_{d+1,d}}{d!} \max_{z \in D} |f^{(d)}(z)|.$$

The above bound has the shortcoming that it depends on the set D, which might be much larger and have less favorable properties than $F(\mathcal{H}_d)$ (which is guaranteed to lie within F(A)), and it shares this drawback with available results from the literature, as, e.g., [5, Theorem 6] and [6, Corollary 2.4]. This is in contrast to experimental evidence reported in [5, 6] as well as in our Example 8.3 below, which suggests that, in many cases, convergence of the sketched FOM approximation is not negatively influenced even when the spectral region of $\mathcal{H}_d + \hat{r}e_d^T$ is significantly larger than that of \mathcal{H}_d . We investigate and explain this phenomenon in detail in the next section.

7 On the error vector and the role of outlying spurious Ritz values

In the previous section we wrote the error between different methods in terms of the "error" vector (see Theorem 5.1)

$$g_w(M)w = \sum_{i=1}^d \alpha_i \beta_i f[M, \lambda_i]w,$$

where $\alpha_i = e_d^T X e_i$, $\beta_i = e_i^T X^{-1} e_1$ with X from the eigenvalue decomposition (16).

The magnitude of the α_i , β_i and of the divided differences needs further analysis. In general, and for large ||w||, we do not expect the eigenvalues of \mathcal{H}_d and $\mathcal{H}_d + we_d^T$ (or H_d and $H_d + we_d^T$) to be close to each other. We now discuss this again in the particular situation of Corollary 6.1, i.e., for $w = \hat{r}$, noting that the derivation works similarly in the other cases.

Letting $\operatorname{dist}(\lambda, F(N)) = \min_{\xi \in F(N)} |\xi - \lambda|$ for any nonzero square matrix N, we define

$$\gamma_{\lambda,N} := \frac{\operatorname{dist}(\lambda, F(N))}{\|N\|}.$$
(34)

This quantity allows us to analyze the contribution of the eigenvalues of $\mathcal{H}_d + \hat{r}e_d^T$ in the error vector. We recall here that the eigenvalues of $\mathcal{H}_d + \hat{r}e_d^T$ are the same as those of $H_d + re_d^T$. As soon as ill-conditioning arises in the generation of the basis U_d , the entries of r start to grow in magnitude. In this case, some of the eigenvalues λ_i may be far from the field of values of \mathcal{H}_d , as $F(\mathcal{H}_d + \hat{r}e_d^T)$ is not included in $F(\mathcal{H}_d)$, whereas others may be either close or within $F(\mathcal{H}_d)$. In the following, we show that whenever ||r|| grows, the quantity β_i is positively affected by becoming correspondingly small, and this is associated with the eigenvalue distance from the field of values of \mathcal{H}_d .

We next assume that $\gamma_{\lambda_i, \mathcal{H}_d} > 1$, that is the eigenvalue λ_i is far from $F(\mathcal{H}_d)$, relative to $\|\mathcal{H}_d\|$. It appears that a significantly distant eigenvalue does not interfere

with the actual error, so that the corresponding term in the sum of g_w becomes negligible, in spite of possibly large values of $f[\mathcal{H}_d, \lambda]$. This argument is justified next.

Remark 7.1 Consider a $d \times d$ lower Hessenberg matrix N with $N_{k,k+1} \neq 0$, for all k, and let $\hat{N} = N + e_d w^*$ for some w. Then for each eigenpair (λ, y) of \hat{N} with ||y|| = 1 it holds, denoting the components $y = (\eta_1, \dots, \eta_d)^T$, that

$$|\eta_{k+1}| \leq \frac{|N_{k,k} - \lambda|}{|N_{k,k+1}|} |\eta_k| + \frac{||N_{k,1:k-1}||}{|N_{k,k+1}|}, \quad k = 1, \dots, d-1,$$

and

$$|(N_{d,d} + w_d) - \lambda||\eta_d| \le ||w_{1:d-1} + N_{d,1:d-1}||.$$

Indeed, let us write $\hat{N}y = \lambda y$. For each row k with $2 \le k < d$ it holds

$$N_{k,k+1}\eta_{k+1} = -(N_{k,k} - \lambda)\eta_k + N_{k,1:k-1}\eta_{1:k-1}.$$

We assume that not all indexed components of y are zero, otherwise the bound follows trivially. Hence,

$$|\eta_{k+1}| \leq \frac{|N_{k,k}-\lambda|}{|N_{k,k+1}|}|\eta_k| + \frac{\|N_{k,1:k-1}\|}{|N_{k,k+1}|}\,\|\eta_{1:k-1}\| \leq \frac{|N_{k,k}-\lambda|}{|N_{k,k+1}|}|\eta_k| + \frac{\|N_{k,1:k-1}\|}{|N_{k,k+1}|}.$$

Let $\phi_k(\lambda) = \prod_{j=1}^k \frac{(N_{j,j} - \lambda)}{N_{j,j+1}}$ be the polynomial of degree k associated with the diagonal and superdiagonal of N.

If
$$^2\operatorname{dist}(\lambda, F(N))/\|N\| = \gamma_{\lambda,N} > 1$$
, then $\frac{|N_{j,j}-\lambda|}{|N_{j,j+1}|} > 1$ for each j , and it holds that $|\eta_{k+1}| \approx |\phi_k(\lambda)|, \qquad k < d.$

This means that the components tend to grow as a power of k, that is

$$|\eta_k| \approx O(\gamma_{\lambda,N}^{k-1}).$$
 (35)

Due to the unit norm of y, this means that if λ is sufficiently far from F(N), the first components of y are tiny, and the subsequent components grow as a growing power of such distance, with the last component of y being O(1) (see Example 5.6). Finally, we observe that the inequality $\frac{|N_{j,j}-\lambda|}{|N_{j,j+1}|} > 1$ for each j may also hold if $|\lambda|$ is much larger than $|N_{j,j}|$ and $|N_{i,i+1}|$; in this case, the increasing property of the components is an intrinsic property of the eigenpair, and it may occur also for λ not far from the field of values of N.

The result outlined in Remark 7.1 is quite general. To apply it to our setting for the error formula, we take $N = \mathcal{H}_d^*$. Except for normalization, $y = y_i$ is the left eigenvector of \mathscr{H}_d corresponding to the eigenvalue λ_i for some i. In particular, $y_i^*e_1 = e_i^T X^{-1}e_1$. If λ_i falls away from the field of values of \mathscr{H}_d^* , the contribution of $\beta_i = e_1^T X^{-1}e_i = (\bar{y}_i)_1$ becomes extremely limited. This property is crucial because it ensures the following counterintuitive result: although the rank-one modification can dramatically affect the spectrum, the wildly varying eigenvalues are not going to contribute to the error.

The following example illustrates the eigenvector growth property.

²A more accurate denominator for the analysis should be $\max_{j} |N_{j,j+1}|$ instead of ||N||. We prefer the latter for clearness, though it leads to a stricter criterion.

Example 7.2 We consider the data in Example 5.6 for fixed d=100, with \mathscr{H}_d^* playing the role of N and $(\mathscr{H}_d+\widehat{r}e_d^T)^*$ that of $N+e_dw^T$. The left plot in Figure 2 shows the spectral quantities associated with the two matrices, including the boundary of $F(\mathscr{H}_d)$. The plot clearly reports the presence of many eigenvalues of $\mathscr{H}_d+\widehat{r}e_d^T$ outside the field of values of \mathscr{H}_d , and also falling into the right half-plane. The right plot shows the components absolute value of the two left eigenvectors of $\mathscr{H}_d+\widehat{r}e_d^T$ corresponding to the eigenvalues pointed to in the left plot. The two additional lines report the values of $|\phi_k(\lambda)|$ for the two eigenvalues; the vectors containing these quantities have been scaled so that the last component has unit value. The eigenvector components behavior is as expected, and it is accurately predicted by the quantity $|\phi_k(\lambda)|$. We notice that the first several components of each eigenvector have a magnitude at the level of machine epsilon. In exact arithmetic their values would follow the steep slope of the other components.

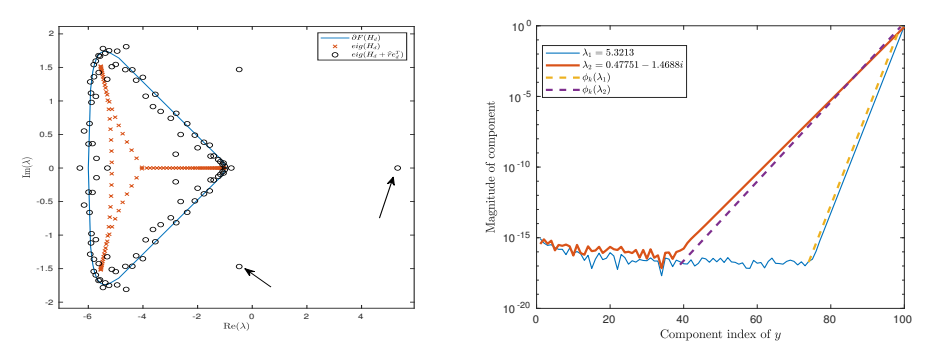


Fig. 2 Example 7.2. Left: field of values and eigenvalues of \mathscr{H}_d , and eigenvalues of $\mathscr{H}_d + \hat{r}e_d^T$. The arrows point to the eigenvalues used in the right plot. Right: absolute values of the eigenvector components for the selected eigenvalues, together with the normalized vector of polynomial values ϕ_k .

It is worth mentioning that whenever β_i is small, the term $\beta_i f[N, \lambda_i]$ remains small. For instance, for the exponential,

$$\beta_i \exp[N, \lambda_i] \approx ||N||^{d-1} (N - \lambda_i I)^{-1} (\exp(N) - \exp(\lambda_i) I) / \operatorname{dist}(F(N), \lambda_i)^{d-1}.$$

We notice that all i's share $||N||^{d-1}$, hence for large $|\exp(\lambda_i)|$ we can focus on controlling the term $|\exp(\lambda_i)|/\operatorname{dist}(F(N),\lambda_i)^{d-1}$. Let us assume, as in the previous example, that $\operatorname{dist}(F(N),\lambda_i) \approx |\lambda_i| > 1$. Then

$$\frac{|\exp(\lambda_i)|}{\operatorname{dist}(F(N), \lambda_i)^{d-1}} \approx \frac{|\exp(\lambda_i)|}{|\lambda_i|^{d-1}}$$

which goes to zero as d goes to infinity.

For our purposes, the analysis above shows that the likely erratic spectral behavior in the sketched approach will not negatively affect the final approximation. Loosely speaking, the matrix structure takes care of purging the undesired eigenvalues. In this way, the "bad" portion of the generated space is implicitly deflated.

Motivated by the analysis above, we return to the relation $\alpha_i \beta_i = \frac{m_d}{\omega'(\lambda_i)}$. Let \mathcal{J} be the set of indexes i such that β_i is not tiny. Hence, the sum over all eigenvalues can be limited to those in \mathcal{J} , that is

$$\sum_{i=1}^{d} \alpha_i \beta_i f[M, \lambda_i] w \approx \sum_{i \in \mathcal{I}} \alpha_i \beta_i f[M, \lambda_i] w.$$

A similar reduction can be written for (21), in terms of the dth order divided differences $f[M, \lambda_1, \ldots, \lambda_d]$, namely $f[M, \lambda_{i_1}, \ldots, \lambda_{i_{|\mathcal{J}|}}]$. Hence, the set \mathcal{J} identifies the "effective" eigenpairs on which the approximation error actually lives.

This shows that bounds relying on approximation properties on the whole field of values $F(\mathcal{H}_d + \hat{r}e_d^T)$ cannot be expected to be fully descriptive of the actual behavior of the method, but that this behavior is rather dictated by a region that is only slightly larger than the spectral region of \mathcal{H}_d .

To formalize this statement, while maintaining the dependence of the convergence on the original problem dimension, we next introduce a more descriptive region of the complex plane than $F(M+we_d^T)$. Let $\delta \geq 0$ be such that all eigenvalues λ_i with $i \in \mathcal{J}$ satisfy $\operatorname{dist}(\lambda, F(M)) < \delta$, and let

$$F(M, \delta) := \{ z \in \mathbb{C} : \operatorname{dist}(z, F(M)) < \delta \};$$

we will call this the *effective* field of values of M. Clearly, $F(M) \subseteq F(M, \delta)$.

For λ_i with $i \notin \mathcal{J}$, we let $\zeta_i = \arg\min_{z \in \partial F(M)} |z - \lambda_i|$. Then we define the following set of values

$$\widehat{\lambda}_i = \left\{ \begin{array}{l} \lambda_i \ i \in \mathcal{J}, \\ \zeta_i \ i \notin \mathcal{J}. \end{array} \right.$$

Then, according to the previous discussion,

$$\sum_{i=1}^d \frac{1}{\omega'(\lambda_i)} f[M,\lambda_i] w \approx \sum_{i=1}^d \frac{1}{\omega'(\widehat{\lambda}_i)} f[M,\widehat{\lambda}_i] w.$$

The definition of the $\widehat{\lambda}_i$ s thus allows us to move (rather than remove) the inactive eigenvalues, while maintaining the number of terms in the divided difference. With these definitions, and using $h(z) := f[z, \widehat{\lambda}_1, \dots, \widehat{\lambda}_d]$, (23) becomes

$$\|h(M)\| \leq (1+\sqrt{2}) \max_{z \in F(M)} |h(z)| \leq (1+\sqrt{2}) \frac{\max_{\zeta \in F(M,\delta)} |f^{(d)}(\zeta)|}{d!}.$$

The bound employs the region of the complex plane where the sketched method is active, and this region can be much smaller than the field of values of $M + we_d^T$. By

means of these new tools, we can obtain an approximate bound of the form

$$||f(M + we_d^T)e_1 - f(M)e_1|| \lesssim m_d(1 + \sqrt{2}) \frac{\max_{\zeta \in F(M,\delta)} |f^{(d)}(\zeta)|}{d!} ||w||,$$
 (36)

which is a family of analogues of (24) depending on the effective field of values, or more precisely on δ .

8 Robust computation of sketched approximations

In this section we want to briefly discuss two further issues related to the experimentally observed numerical (in)stability of sketched Krylov methods. On the one hand, we provide arguments that partially explain why the WS-Arnoldi version (15) of the sFOM approximation typically appears to be very robust in floating point arithmetic despite the inversion of the possibly very ill-conditioned matrix T_d that is involved. On the other hand, we explain which potential problems can occur with the non-whitened variant (14) based on a rank-one modification of H_d .

Remark 8.1 Concerning the floating-point behavior of the whitened-sketched version (15) of sFOM, Proposition 3.2 shows that the implicit transformation $U_dT_d^{-1}$ makes the non-orthogonal basis U_d incredibly well-conditioned. However, it comes at the price of inverting T_d on the coefficient vector $\hat{y} = f(\hat{H}_d + \hat{t}e_d^T)e_1$ of the sketched FOM approximation. Luckily, this inversion can be expected to be numerically much more stable than the possibly very large condition number of T_d suggests at a first sight. It is well-known, see, e.g., [27], that the entries of $f(H)e_1$, where H is a Hessenberg matrix, often decay geometrically from top to bottom (with the precise rate of decay depending both on the function f and the spectral region of H). Therefore, later entries of the vector typically quickly become tiny. This is relevant in our setting as the potential ill-conditioning in T_d^{-1} is "structured": The non-orthogonal basis U_d gradually becomes more ill-conditioned as the iteration progresses and (almost) linear dependence occurs mostly between "later" basis vectors. To understand this, consider the extreme case of no orthogonalization at all: Then, the sequence of Krylov basis vectors converges towards the dominant eigenvector of A, so that later basis vectors will all point in almost the same direction, while staying well linearly independent from the first basis vectors. A similar phenomenon is preserved when employing a partial orthogonalization with small truncation parameter.

As the sketching matrix S distorts inner products in a controlled manner due to (3), this property of U_d is inherited by the sketched basis SU_d for which we perform the QR decomposition. This observation implies that the severe ill-conditioning of T_d is mostly encoded in a bottom right subblock. Therefore, when computing $T_d^{-1}\hat{y}$, the most ill-conditioned part of T_d acts on the very tiny last entries of \hat{y} . While the results of the corresponding computations might be completely spoiled by large relative errors, these errors do not heavily influence the first, larger entries. Note, however, that spoiled results for the small later entries of \hat{y} might mean that the final attainable accuracy of the sketched approximation is limited.

Remark 8.2 Considering (14), note that the matrix $H_d + re_d^T$ is often not well-balanced, in the sense that the norm of its last column is typically much larger than that of all other columns. It is known since the 1970s that balancing can have an influence on the

approximation accuracy for matrix functions; e.g., when using techniques such as Padé approximation [28, 29], although the effect is difficult to rigorously quantify; cf., e.g., [30, Sections 3, 6].

We turn to the specific case of scaling-and-squaring methods for the matrix exponential. A first step in such methods is the computation of a parameter γ such that $\|2^{-\gamma}(H_d+re_d^T)\| < 1$. When $H_d+re_d^T$ is poorly balanced, the value of γ will be almost solely determined by its last column, and the entries of all other columns in $2^{-\gamma}(H_d+re_d^T)$ might become tiny. This and related effects are known under the term *overscaling* in the matrix function literature; see, e.g., [31, Section 1] or [32]. Clearly, this can result in a noticeable decrease in the accuracy of the method in the presence of round-off error. In contrast, the matrix $\hat{H}_d + \hat{t}e_d^T$ from (14) will typically be better balanced due to the similarity transformation with T_d and thus less prone to overscaling effects.

Example 8.3 We report the results of an illustrative example. Here, A is obtained by discretizing the convection-diffusion operator

$$\mathcal{L}(u) = -\nu \Delta u + \vec{w} \cdot u, \tag{37}$$

on the unit square $[0,1]^2$ by centered finite differences. We use viscosity parameter $\nu=10^{-2}$, the convection field $\vec{w}=(\frac{3}{2}y(1-x^2),-3x(1-y^2))$ and N=50 discretization points in each spatial direction. The resulting matrix A is highly non-normal with extremely ill-conditioned eigenvector basis, $\kappa(X)\approx 1.5\cdot 10^{22}$. We aim to approximate the action of the matrix exponential $\exp(-A)b$, where b is the normalized vector of all ones.

We begin by comparing different possible implementations of sFOM, using a truncation parameter k=2 in the generation of the non-orthogonal Krylov basis U_d and a sketching dimension s=400. Specifically, we compare the whitened-sketched sFOM approximation (15) with the version (14) based on the rank one modification $H_d + re_d^T$. Due to the bad balancing of $H_d + re_d^T$, the computation of $\exp(H_d + re_d^T)$ might be extremely sensitive to round-off, also depending on which algorithm is used for the matrix exponential; cf. also the discussion in Remark 8.2. We therefore compare two different versions: One which directly uses the built-in MATLAB function $\exp(w)$ (which implements the scaling-and-squaring method from [31]) and one which first computes a Schur decomposition of A and then applies $\exp(w)$ only to the triangular factor. Note that this can lead to better numerically stability for two reasons: First, the triangular factor of the Schur decomposition will in general be better balanced than $H + re_d^T$, and second, $\exp(w)$ contains several implementation tricks to specifically improve the behavior for triangular inputs; see [31, Section 2]. For the whitened-sketched Arnoldi method, due to the better balancing, using either $\exp(w)$ directly or working with a Schur decomposition gives virtually identical results so that we do not report separate curves here.

The results of this experiment are depicted on the left-hand side of Figure 3. It can be clearly observed that the whitened-sketched method closely follows the convergence of the full Arnoldi method, with only a very small deviation towards the end of the process. In contrast, both versions of sFOM based on the rank-one modification (14) show signs of instability. While all sketched methods behave identical for the first 90 iterations, the version based on expm becomes very unstable after that and shows increasing/stagnating error norms for about 50 iterations before continuing to converge after that. The version based on the Schur decomposition longer behaves similarly to the whitened-sketched method, but also starts to deviate around the 130th iteration, when reaching a relative error norm of about 10^{-8} .

It is a common conception (see, e.g., [7]) that convergence of sketched methods typically deteriorates once the non-orthogonal basis becomes numerically linearly dependent (i.e., once it has a condition number larger than $\varepsilon_{machine}^{-1}$, the reciprocal of the unit round-off). Our

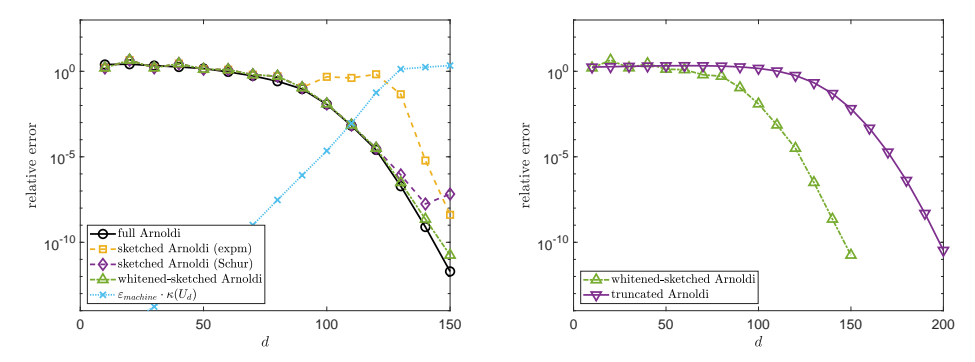


Fig. 3 Left: Comparison of different versions of the sFOM approximation with full Arnoldi for approximating the action of the matrix exponential. The conditioning of the non-orthogonal Krylov basis U_d is also depicted. Right: Comparison of "best" sFOM implementation (i.e., whitened-sketched) with truncated Arnoldi. In both cases, the truncation parameter is k=2 and the sketching parameter is k=400.

experiment clearly reveals that this is not necessarily true and that there are also other factors which have an influence. For sFOM using expm, stability problems occur long before the basis becomes severely ill-conditioned, and the whitened-sketched method continues to converge smoothly also once this happens. Only for sFOM using a Schur decomposition, the linear dependence of the basis and occurrence of stability problems coincide.

In the right part of Figure 3, we compare the best performing of the sFOM variants, i.e., the whitened-sketched version (15), to truncated Arnoldi (12) using the same truncation parameter k=2. We can observe that in truncated Arnoldi, convergence is significantly delayed. In the initial 110 iterations of the method, a plateau of stagnating (or even slightly increasing) error norms occurs. After that, convergence begins, and the convergence rate is only slightly slower than that of the full (and whitened-sketched) method. The truncated method reaches the target relative error norm 10^{-11} after 200 iterations. Thus, the sketched-whitened method uses 25% fewer matrix-vector products in this case.

9 Conclusions

We have provided a new analysis of sketched Krylov subspace methods. In particular, we have derived a new *sketched Arnoldi relation*, which applies to any Krylov method that combines subspace embeddings with a truncated orthogonalization process. This relation can be used to obtain new insights into the behavior of these methods and better explains some phenomena that are frequently observed, e.g., that methods continue to perform well even if they produce spurious Ritz values far outside the field of values of A.

To demonstrate this, we have specifically focused on the application of sketching to the approximation of f(A)b, the action of a matrix function on a vector. We have derived new formulas for expressing certain rank-one modifications of a matrix function via divided differences and then used those to compare sketched and truncated Krylov approximations to the standard (full) Arnoldi approximation. In particular, we could prove that for functions like the exponential, for growing Krylov dimension

d, the sketched Arnoldi approximation is guaranteed to converge to the full Arnoldi approximation, and the nature of our bound suggests that one can expect this convergence to take place at roughly the same speed as convergence of the full Arnoldi approximation to f(A)b.

To provide the reader with an overall picture, the following table summarizes our main matrix function approximations, in the truncated and fully orthonormal bases. Among the various sketched forms we have discussed, we report here only those that appear to be most reliable for practical purposes.

approx	truncated basis U_d		fully orthonormal basis \mathcal{U}_d	
$f_d^{\scriptscriptstyle ext{FOM}}$	-		$\mathscr{U}_d f(\mathscr{H}_d) e_1 \ b\ $	(11)
$f_d^{\scriptscriptstyle { m TR}}$	$U_d f(H_d) e_1 \ b\ $	(12)		(31)
$f_d^{ ext{SK}}$	$U_d T_d^{-1} f\left(\widehat{H}_d + \widehat{t} e_d^T\right) e_1 \ Sb\ $	(15)	$\mathcal{U}_d f(\mathscr{H}_d + \widehat{r} e_d^T) e_1 \ b\ $	(28)

For a matrix analysis, the truncated-Arnoldi form of the sketched approximation, namely $f_d^{SK} = U_d f \left(H_d + r e_d^T \right) e_1 ||b||$, would have several advantages. However, we have illustrated that this form may showcase a quite erratic numerical behavior, compared with the stabilized one reported in the table.

For studying the a-priori error with respect to the ideal FOM approximation, writing the truncated and the sketched approximations in terms of the fully orthonormal basis \mathcal{U}_d (third column in the table) leads to more insightful formulas. It should be kept in mind, however, that in our setting the formulation of sketched and truncated approximations via the fully orthonormal basis is not computationally affordable.

Our focus in this work was on deepening the theoretical understanding of existing sketching approaches, not on introducing new algorithmic concepts. Therefore, we did not perform extensive, large-scale numerical experiments, as thorough experimental studies illustrating the potential of sketched Krylov methods for matrix functions already exist in the literature; see, e.g., [5, 6].

In a forthcoming paper, we will employ the sketched Arnoldi approximation derived here for analyzing and implementing sketched and truncated Krylov subspace methods for efficiently solving matrix Sylvester and Lyapunov equations.

Acknowledgments

The first and third authors are members of the INdAM Research Group GNCS that partially supported this work through the funded project GNCS2022 "Tecniche Avanzate per Problemi Evolutivi: Discretizzazione, Algebra Lineare Numerica, Ottimizzazione" (CUP_E55F22000270001).

References

[1] Halko, N., Martinsson, P.-G., Tropp, J.A.: Finding structure with randomness:

- Probabilistic algorithms for constructing approximate matrix decompositions. SIAM Rev. **53**(2), 217–288 (2011)
- [2] Sarlos, T.: Improved approximation algorithms for large matrices via random projections. In: 47th Annual IEEE Symposium on Foundations of Computer Science (FOCS'06), pp. 143–152 (2006). IEEE
- [3] Woolfe, F., Liberty, E., Rokhlin, V., Tygert, M.: A fast randomized algorithm for the approximation of matrices. Appl. Comput. Harmon. Anal. **25**, 335–366 (2008)
- [4] Balabanov, O., Grigori, L.: Randomized Gram-Schmidt process with application to GMRES. SIAM J. Sci. Comput. 44(3), 1450–1474 (2022)
- [5] Cortinovis, A., Kressner, D., Nakatsukasa, Y.: Speeding up Krylov subspace methods for computing f(A)b via randomization. arXiv preprint arXiv:2212.12758 (2022)
- [6] Güttel, S., Schweitzer, M.: Randomized sketching for Krylov approximations of large-scale matrix functions. arXiv preprint arXiv:2208.11447 (2022)
- [7] Nakatsukasa, Y., Tropp, J.A.: Fast & accurate randomized algorithms for linear systems and eigenvalue problems. arXiv preprint arXiv:2111.00113 (2021)
- [8] Lanczos, C.: An iteration method for the solution of the eigenvalue problem of linear differential and integral operators. J. Res. Natl. Stand. 45, 255–282 (1950)
- [9] Balabanov, O., Nouy, A.: Randomized linear algebra for model reduction. Part I: Galerkin methods and error estimation. Adv. Comput. Math. 45(5), 2969–3019 (2019)
- [10] Timsit, E., Grigori, L., Balabanov, O.: Randomized orthogonal projection methods for Krylov subspace solvers. arXiv preprint arXiv:2302.07466 (2023)
- [11] Simoncini, V.: Computational methods for linear matrix equations. SIAM Rev. **58**(3), 377–441 (2016)
- [12] The MathWorks, Inc.: MATLAB 7, R2020b edn. (2020). The MathWorks, Inc.
- [13] Arnoldi, W.E.: The principle of minimized iteration in the solution of the matrix eigenvalue problem. Q. Appl. Math. 9, 17–29 (1951)
- [14] Carson, E., Lund, K., Rozložník, M., Thomas, S.: Block Gram-Schmidt algorithms and their stability properties. Linear Algebra Appl. **638**, 150–195 (2022)
- [15] Martinsson, P.-G., Tropp, J.A.: Randomized numerical linear algebra: Foundations and algorithms. Acta Numer. 29, 403–572 (2020)

- [16] Sohler, C., Woodruff, D.P.: Subspace embeddings for the L1-norm with applications. In: Proceedings of the Forty-third Annual ACM Symposium on Theory of Computing, pp. 755–764 (2011)
- [17] Ilić, M., Turner, I.W., Simpson, D.P.: A restarted Lanczos approximation to functions of a symmetric matrix. IMA J. Numer. Anal. **30**(4), 1044–1061 (2010)
- [18] Boor, C.: Divided differences. Surv. Approx. Theory 1, 46–69 (2005)
- [19] Beckermann, B., Kressner, D., Schweitzer, M.: Low-rank updates of matrix functions. SIAM J. Matrix Anal. Appl. **39**(1), 539–565 (2018)
- [20] Curtiss, J.H.: Limits and bounds for divided differences on a Jordan curve in the complex domain. Pacific J. Math. **12**(4), 1217–1233 (1962)
- [21] Eiermann, M., Ernst, O.G.: A restarted Krylov subspace method for the evaluation of matrix functions. SIAM J. Numer. Anal. 44(6), 2481–2504 (2006)
- [22] Tal-Ezer, H.: On restart and error estimation for Krylov approximation of w = f(A)v. SIAM J. Sci. Comput. **29**(6), 2426–2441 (2007)
- [23] Crouzeix, M., Palencia, C.: The numerical range is a $(1+\sqrt{2})$ -spectral set. SIAM J. Matrix Anal. Appl. **38**(2), 649–655 (2017) https://doi.org/10.1137/17M1116672 https://doi.org/10.1137/17M1116672
- [24] Higham, N.J.: Functions of Matrices: Theory and Computation. SIAM, Philadel-phia (2008)
- [25] Horn, R.A., Johnson, Ch.R.: Topics in Matrix Analysis. Cambridge University Press, Cambridge (1991)
- [26] Gallopoulos, E., Saad, Y.: Efficient solution of parabolic equations by Krylov approximation methods. SIAM J. Sci. Stat. Comput. 13(5), 1236–1264 (1992)
- [27] Pozza, S., Simoncini, V.: Inexact Arnoldi residual estimates and decay properties for functions of non-Hermitian matrices. BIT **59**(4), 969–986 (2019)
- [28] Fair, W., Luke, Y.L.: Padé approximations to the operator exponential. Numer. Math. 14(4), 379–382 (1970)
- [29] Ward, R.C.: Numerical computation of the matrix exponential with accuracy estimate. SIAM J. Numer. Anal. **14**(4), 600–610 (1977)
- [30] Al-Mohy, A.H., Higham, N.J.: Computing the action of the matrix exponential, with an application to exponential integrators. SIAM J. Sci. Comput. **33**(2), 488–511 (2011)
- [31] Al-Mohy, A.H., Higham, N.J.: A new scaling and squaring algorithm for the

matrix exponential. SIAM J. Matrix Anal. Appl. $\mathbf{31}(3),\,970–989$ (2010)

[32] Dieci, L., Papini, A.: Padé approximation for the exponential of a block triangular matrix. Linear Algebra Appl. $\bf 308 (1-3), \, 183-202 \, (2000)$